Available online at www.sciencedirect.com

ScienceDirect

St. Petersburg Polytechnical University Journal: Physics and Mathematics 1 (2015) 436–443

www.elsevier.com/locate/spjpm

The sensitivity of the adaptive algorithm with a posteriori error control to marking criteria

Maria A. Churilova

Peter the Great St. Petersburg Polytechnic University, 29 Politekhnicheskaya St., St. Petersburg 195251, Russian Federation

Available online 28 January 2016

Abstract

The aim of this work is to compare different marking strategies, their influence on the work of adaptive algorithms with a posteriori error control for plane elasticity problems. The error control was performed using a functional error majorant. The implemented adaptive algorithms were based on the functional error majorant with no symmetry limitation on the free tensor, computed using the zero-order Raviart–Thomas approximations on triangular meshes. The four most commonly used element-marking criteria were used in adaptation. Numerical results for several plane-strain problems have been presented, including the case of different materials and geometry. A comprehensive analysis of the obtained results was given.

Keywords: A posteriori error estimate; Linear elasticity; Adaptive algorithm; Raviart–Thomas approximation.

1. Introduction

The paper discusses functional a posteriori error estimates for two-dimensional problems of linear elasticity theory. These estimates were first studied numerically in Ref. [1]. They were initially derived based on the relations of the duality theory of calculus of variations; this method was suggested in Ref. [2]. Later, Monograph [3] obtained the same estimates using the transformation of integral identities. Ref. [1] also discussed particular cases of estimates for a number of two-dimensional problems: plane strain, plane stress and axisymmetrical case.

The literature describes two types of functional error majorants for these problems: those explicitly and implicitly taking into account the symmetry of the free tensor that is a part of the estimate. Estimates of the second type allow using special finite elements developed for mixed methods. This approach was first suggested and implemented in Ref. [4].

Numerical studies of the functional approach to solving plane problems of linear elasticity theory were carried out by several authors. For example, Ref. [1] cites two examples of solving plane-strain problems with adapting the computational mesh in complexly shaped areas; in this case, the 'symmetrical' estimate and, respectively, the continuous piecewise-linear approximation of the finite-element method are used. The efficiency index of the estimate (i.e., the ratio of the error majorant to the estimated norm, the optimal index value is unity) increased, according to the results. The study [4] demonstrated that error overestimation increases for quadrilateral

E-mail address: m_churilova@mail.ru.

http://dx.doi.org/10.1016/j.spjpm.2016.01.001

(Peer review under responsibility of St. Petersburg Polytechnic University).

finite-element meshes: for some problems, the efficiency index exceeds the optimal value by about an order of magnitude on a mesh containing a total of several thousands of nodes. Refs. [4,5] used the zero-order Raviart–Thomas approximation and the Arnold–Boffi–Falk approximation with two additional degrees of freedom on each element for computing the functional majorants on nested quadrilateral meshes without adaptation. Aside from that, Ref. [6] studied the main theoretical properties and the aspects of practically implementing both types of functional a posteriori estimates, and listed the numerical results obtained by the adaptive algorithms for solving plane-strain problems. The theorems on the computational properties of the estimates and the corresponding error indicators have been formulated and proved.

The goal of this study is to perform a comparative analysis of various methods for selecting the elements for splitting (element marking) and the influence of these methods on the output of the mesh adaptation algorithm (the adaptive algorithm). Effectively, the study continues the research in [6] and takes as a basis some ideas from Monograph [7].

2. Problem setting

A plane problem of linear elasticity theory in the $\Omega \subset \mathrm{R}^2$ region with a Lipschitz -continuous boundary B consisting of two parts B_1 and B_2 has the form

$$\begin{cases} \sigma = L\varepsilon(u) & \text{in } \Omega \\ \mathrm{Div}\sigma + f = 0 & \text{in } \Omega \\ u = u_0 & \text{at } B_1 \\ \sigma n = F & \text{at } B_2 \end{cases}, \tag{1}$$

where Div is the tensor divergence.

The unknown is a vector displacement field $u(x_1,x_2)$ through which the strain tensor

$$\varepsilon(u) = \frac{1}{2}\left(\nabla u + (\nabla u)^T\right)$$

and the stress tensor σ are expressed.

The body force vector

$$f \in \mathrm{L}_2(\Omega, \mathrm{R}^2) = \mathrm{L}_2(\Omega) \times \mathrm{L}_2(\Omega),$$

the normal stresses $F \in \mathrm{L}_2(B_2,\mathrm{R}^2)$ on a part of the boundary B_2, and also the displacements $u_0 \in \mathrm{W}_2^1(\Omega,\mathrm{R}^2)$ at B_1 are given. The Lebesgue space L_2 is a space of square-integrable functions. The Sobolev space W_2^1 is a space of functions from L_2 whose generalized derivatives also belong to L_2. The vector n is the unit normal to B_2, L is the elastic constant tensor. It is assumed that there are positive constants λ_1 and λ_2 for the tensor L, such that

$$\lambda_1^2|\varepsilon|^2 \le L\varepsilon : \varepsilon \le \lambda_2^2|\varepsilon|^2 \tag{2}$$

for each tensor $\varepsilon \in \mathrm{M}_{sym}^{2\times 2}$, where $\mathrm{M}_{sym}^{2\times 2}$ is the space of symmetric second-order tensors of dimension 2. It is also assumed that the symmetry condition

$$L_{ijkm} = L_{jikm} = L_{kmij}, L_{ijkm} \in \mathrm{L}_\infty(\Omega),$$
$$i, j, k, m = 1, 2,$$

where the Lebesgue space $\mathrm{L}_\infty(\Omega)$ consists of functions bounded almost everywhere in Ω, is satisfied.

The solution of the problem (1) is sought for in the generalized sense:

Find the function u *from* $\mathrm{V} = u_0 + \mathrm{V}_0$, *where* $\mathrm{V}_0 = \{w \in \mathrm{W}_2^1(\Omega,\mathrm{R}^2) \,|\, w = 0$ *at* $B_1\}$, *satisfying the integral relation*

$$\int_\Omega L\varepsilon(u) : \varepsilon(w)d\Omega = \int_\Omega f \cdot wd\Omega + \int_{B_2} F \cdot wdB \tag{3}$$

for any $w \in \mathrm{V}_0$.

Let $v \in \mathrm{V}$ be some approximate solution of the problem (3). In order to control the accuracy of the solution v, it is necessary to have an upper estimate for the energy norm

$$|||u - v||| := \left(\int_\Omega L\varepsilon(u - v) : \varepsilon(u - v)d\Omega\right)^{1/2}.$$

Ref. [1] obtained for the problem (1) a functional error majorant:

$$|||u - v||| \le C\left(\|\mathrm{Div}\tau + f\|_\Omega^2 + \|\tau n - F\|_{B_2}^2\right)^{1/2} + \\ + |||\tau_{sm} - L\varepsilon(v)|||_* + \frac{C_{\Omega B_1}}{\lambda_1}\|\tau_{sk}\|_\Omega, \tag{4}$$

where $\|...\|_\Omega$ and $\|...\|_{B_2}$ are the norms in L_2; τ is an arbitrary tensor from the Hilbert space

$$H = \left\{\begin{matrix} \tau \in \mathrm{L}_2(\Omega, \mathrm{M}^{2\times 2})| \\ \mathrm{Div}\tau \in \mathrm{L}_2(\Omega, \mathrm{R}^2), \\ \tau n \in \mathrm{L}_2(B_2, \mathrm{R}^2) \end{matrix}\right\};$$

τ_{sm} and τ_{sk} are the symmetric and the skew-symmetric parts of the tensor τ, respectively; $C_{\Omega B_1}$ is the constant from Korn's inequality that can be estimated numerically.

The auxiliary norm in the majorant is computed by the formula

$$|||\tau|||_* = \left(\int_\Omega L^{-1}\tau : \tau dx\right)^{1/2}.$$

The constant C must satisfy the inequality

$$\int_{\Omega} |w|^2 d\Omega + \int_{B_2} |w|^2 dB \le C^2 |||w|||^2$$

for each $w \in V_0$.

By twice applying the Cauchy inequality with a parameter to the majorant (4), we can obtain a quadratic structure of the majorant that is more convenient for computations:

$$\begin{aligned} &|||u - v|||^2 \le M^2(v, \tau, \beta_1, \beta_2) := \\ &:= (1 + \beta_1) |||\tau_{sm} - L\varepsilon(v)|||_*^2 + \\ &+ \left(1 + \frac{1}{\beta_1}\right)(1 + \beta_2) C^2 \|\mathrm{Div}\tau + f\|_{\Omega}^2 + \\ &+ \left(1 + \frac{1}{\beta_1}\right)(1 + \beta_2) C^2 \|\tau n - F\|_{B_2}^2 + \\ &+ \left(1 + \frac{1}{\beta_1}\right)\left(1 + \frac{1}{\beta_2}\right)\left(\frac{C_{\Omega B_1}}{\lambda_1}\right)^2 \|\tau_{sk}\|_{\Omega}^2, \end{aligned} \tag{5}$$

where $\beta_1 > 0$, $\beta_2 > 0$ are arbitrary parameters.

The formulae for the optimal values of β_1 and β_2 at fixed τ and for the C constant are listed in Ref. [6].

Significantly, the majorant in the inequality (5) is accurate, as the equality of the right and the left-hand sides is achieved by substituting $\tau = \sigma$ and $\beta_1 = 0$ into it.

In this study, the functional majorant (5) is implemented based on the assumption of isotropic linear elasticity: the elastic constant tensor L depends on two parameters of the material, namely, on Young's modulus E and on Poisson's ratio ν.

To compute the majorant $M(v,\tau,\beta_1,\beta_2)$, it is necessary to select the type of approximation for the tensor field τ. The positive results of the studies [4–6] make it reasonable to apply the zero-order Raviart–Thomas approximation. The first summand of the majorant on each element of the mesh T:

$$\eta_T = \left(\int_T (L^{-1}\tau - \varepsilon(u_h)) : (\tau - L\varepsilon(u_h)) dT\right)^{1/2}$$

is used as an error indicator for the approximate solution $v = u_h$, obtained on a finite-element mesh with a characteristic size h. From now on, let us denote the majorant-based indicator by η_T^{RT}, since the Raviart–Thomas approximation is used to compute it.

A reference indicator

$$\eta_T^{ref} = \left(\int_T L\varepsilon(u_{ref} - u_h) : \varepsilon(u_{ref} - u_h) dT\right)^{1/2},$$

where u_{ref} is the reference solution, is used to estimate the quality of adaptive meshes. As such, an approximate solution obtained on a mesh with a characteristic size $h/4$ was selected; the mesh was obtained from the initial one by uniformly splitting the elements.

The relative error

$$e = \frac{|||u_h - u_{ref}|||}{|||u_{ref}|||} \cdot 100\%$$

and the efficiency index of the majorant

$$I_{eff} = \frac{M(u_h, \tau, \beta_1, \beta_2)}{|||u_h - u_{ref}|||},$$

are computed through the reference solution and then used to control the quality of the estimates obtained during the study.

3. Element marking criteria

During mesh adaptation, a criterion for selecting the elements for splitting at each step of the algorithm should be chosen (see, for example, Monograph [8] and Book [9]). From a mathematical standpoint, it can be represented by the operator $m(\eta_T)$ transforming the values array of the error indicator into an array of zeros and unities (0 – the element is not split, 1 – the element is split). Let us call such an operator a marker. Using different markers produces different mesh sequences, so the resulting adaptive meshes may be significantly dissimilar. Four of the most commonly used markers were chosen for comparative analysis.

1. The maximum value marker $m_1(\eta_T)$: all elements for which

   $$\eta_T > \alpha \max_{i=1\ldots N_t}(\eta_{T_i})$$

   are split, where N_t is the number of elements in the mesh; $\alpha \in (0;1)$ is a constant, typically set to equal 0.5.

2. The mean value marker $m_2(\eta_T)$: all elements for which

   $$\eta_T > \left(\sum_{i=1}^{N_t} \eta_{T_i}\right)/N_t$$

   are split.

3. The $m_3(\eta_T)$ marker sets the splitting of the given number of elements with the maximum error, for which purpose it is necessary to sort the elements by descending indicator value.
4. The $m_4(\eta_T)$ marker, or the bulk criterion: the first k elements with the maximum error are split, for which

   $$\sum_{i=1}^{k} \eta_{T_i} \ge \alpha \sum_{i=1}^{N_t} \eta_{T_i} > \sum_{i=1}^{k-1} \eta_{T_i},$$

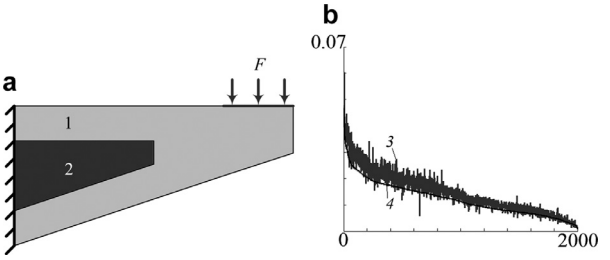

Fig. 1. A loaded structure (computational domain) with varying material parameters (a) and the corresponding plot for the values of the error indicators η^{ref} (4) and η^{RT} (3) depending on the element number (b). The materials are concrete (1) and steel (2). Example 1 is illustrated.

where $\alpha \in (0;1)$ is some constant. For this marker it is also necessary to sort the elements by descending indicator value.

In order to compare various markers, Monograph [7] suggested computing 'marker accuracy':

$$\mu = \left(1 - \frac{\left\| m(\eta_T) - m(\eta_T^{ref}) \right\|_1}{N_t}\right) \cdot 100\%,$$

where $\|x\|_1 = \sum_i |x_i|$ is the 1-norm of the vector.

The quantity μ allows to estimate how close the number and the location of the elements selected with the given marker are to each other when using the indicator η_T and the reference indicator η_T^{ref}.

4. Examples of adaptive algorithms working

Let us discuss several examples demonstrating how adaptive algorithms work with different markers for solving plane-strain problems; let us then analyze whether the functional approach is stable against changing the marking criterion. In all cases the adaptation starts with a uniform mesh with a relatively small number of nodes, and ends as soon as the given level of relative error e, equal to 3–4%, is reached.

Example 1. Let us examine some structure whose computational domain is shown in Fig. 1(a); it consists of two parts with different material parameters:

concrete $\ldots\ldots\ldots E = 30\,\mathrm{GPa}, \quad \nu = 0.2;$
steel $\ldots\ldots\ldots E = 210\,\mathrm{GPa}, \quad \nu = 0.3.$

The left end of the structure is fixed; a distributed load $F = 10^8\,\mathrm{N/m^2}$ is applied to a part of the upper boundary.

Fig. 1(b) shows a plot for the value distribution of the error indicators η^{ref} and η^{RT} on a uniform mesh consisting of 2000 elements. The numbers of the elements of the abscissa axis are sorted by descending reference indicator value. The plot demonstrates that the majorant-based indicator reproduces the key features of the error distribution in the region.

Table 1
The results of the adaptive algorithms work.

Marker	μ (%)	N_s	N_n	e(%)	I_{eff}
Example 1 (the reference mesh contains 10334 nodes, $e=3.00\%$)					
m_1	97.85	8	12204	2.83	1.43
m_2	94.70	6	30007	1.89	1.43
m_3	92.80	6	12277	2.86	1.42
m_4	93.40	9	16880	2.47	1.43
Example 2 (the reference mesh contains 6039 nodes, $e=3.00\%$)					
m_1	99.79	9	10670	2.83	1.37
m_2	77.50	5	22205	1.02	1.41
m_3	88.75	5	12420	2.76	1.37
m_4	86.25	8	13701	2.47	1.40
Example 3 (the reference mesh contains 10430 nodes, $e=3.99\%$)					
m_1	99.57	15	14499	3.54	1.65
m_2	91.28	6	41566	3.95	1.95
m_3	79.65	6	36096	4.00	1.94
m_4	79.65	8	15493	3.77	1.76

Fig. 2 shows a uniform mesh with the elements selected for splitting using the four above-described markers computed by the η^{RT} indicator. Similar plots, constructed for the reference indicator, are shown in order to estimate whether the elements have been selected correctly. From now on, we are going to split 30% of the elements with the maximum error for the m_3 marker; a parameter value $\alpha = 0.3$ was selected for the m_4 marker.

The accuracy of the markers on a uniform mesh is listed in the second column on Table 1. Fig. 3 shows the nodes of adaptive meshes obtained at the final step of the algorithms (the adaptation started with a uniform mesh with 282 nodes) To compare the quality of meshes, a reference mesh was constructed using the η^{ref} indicator. 25 elements with the maximum error were split at each step of the adaptation algorithm. It took 105 adaptation steps to achieve the desired error $e \leq 3\%$ on the reference mesh. This procedure was used exclusively for the computing experiment, since it requires too many resources in real computations.

The number of mesh nodes N_n, the relative error e and the majorant's efficiency index I_{eff} for each marker on the final adaptive meshes are listed in Table 1, where N_s denotes the number of steps in the adaptive algorithm, the stopping criterion is $e \leq 3\%$.

Let us note that the efficiency index of the computed majorant virtually does not depend on the

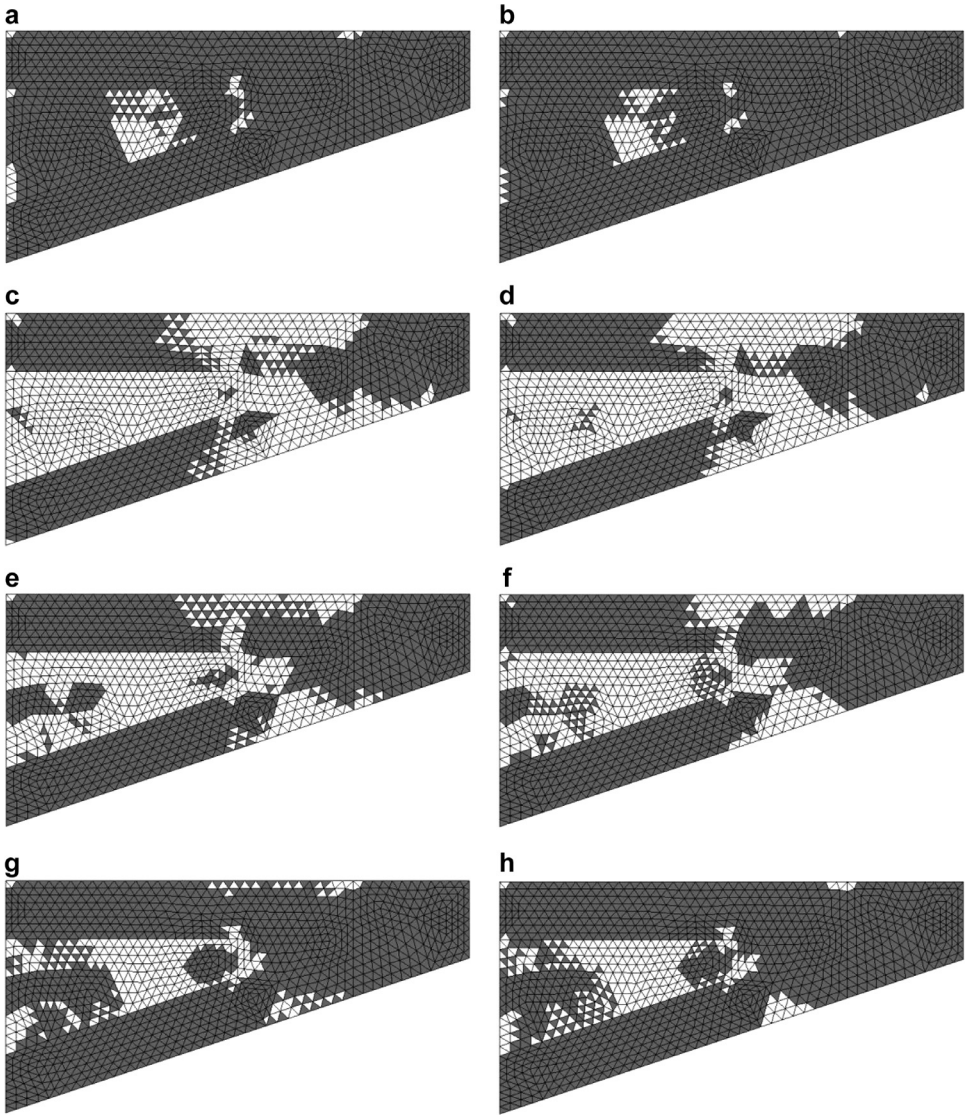

Fig. 2. The elements of the domain (see Fig. 1 (a)) selected for splitting (lightly shaded) using different markers: $m_1(\eta_T^{ref})$ (a), $m_1(\eta_T^{\mathrm{RT}})$ (b); $m_2(\eta_T^{ref})$ (c), $m_2(\eta_T^{\mathrm{RT}})$ (d); $m_3(\eta_T^{ref})$ (e), $m_3(\eta_T^{\mathrm{RT}})$ (f); $m_4(\eta_T^{ref})$ (g), $m_4(\eta_T^{\mathrm{RT}})$ (h). Example 1 is illustrated.

marking criterion, i.e., the accuracy of the global estimate remains unaffected. It can be also seen from Table 1 that the m_2 marker leads to excessive mesh splitting; it produces three times as many nodes as the reference mesh. Using the m_4 marker results in the highest number of algorithm steps for this example.

Example 2. Let us examine another structure whose computational domain is shown in Fig. 4(a); it consists of three parts, with the left end fixed; a distributed load $F = 10^7$ N/m^2 is applied to the right end. Fig. 4(c)–(f) shows nodes of the adaptive meshes at the final step of the algorithms obtained with different markers. The nodes of the reference mesh are shown in Fig. 4(b). The accuracy of the markers on a uniform mesh with 1344 nodes is listed in the second column of Table 1. Fig. 5 shows a uniform mesh with the elements selected for splitting using the markers computed by the indicators η^{RT} and η^{ref}.

The number of nodes, the relative error and the efficiency index of the majorant for each marker on the resulting adaptive meshes are listed in Table 1 in the respective cells. The stopping criterion for the

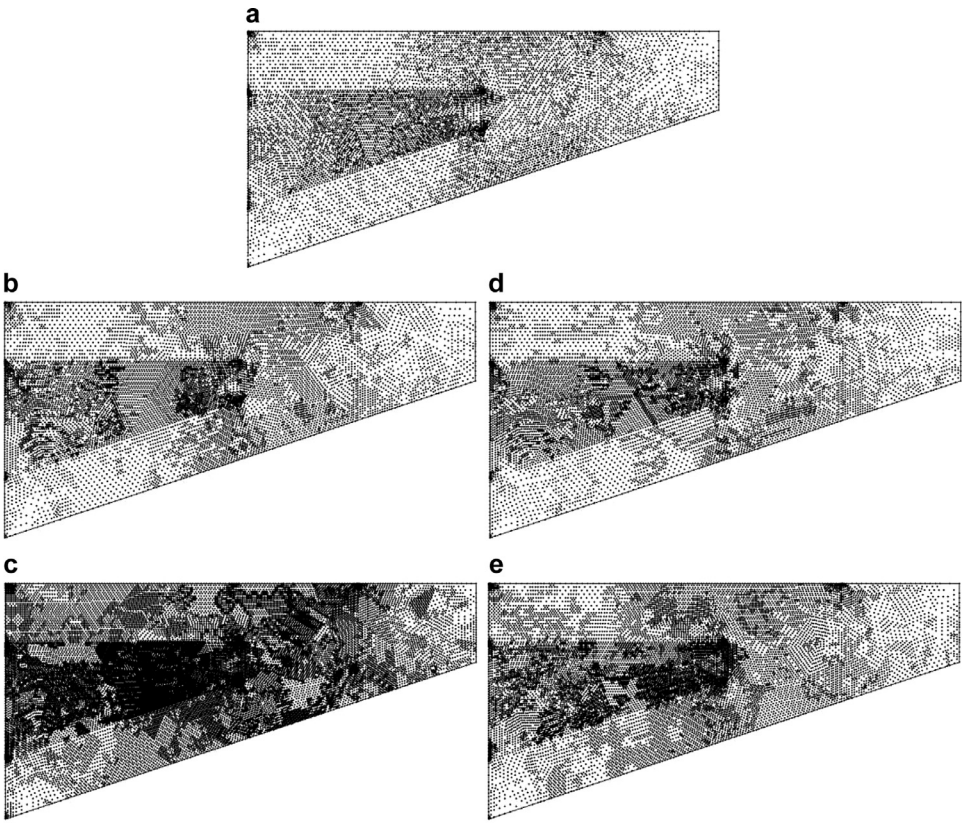

Fig. 3. The resulting nodes of finite-element meshes obtained using the markers m_1 (b), m_2 (c), m_3 (d), m_4 (e), and the reference mesh (a). Example 1 is illustrated.

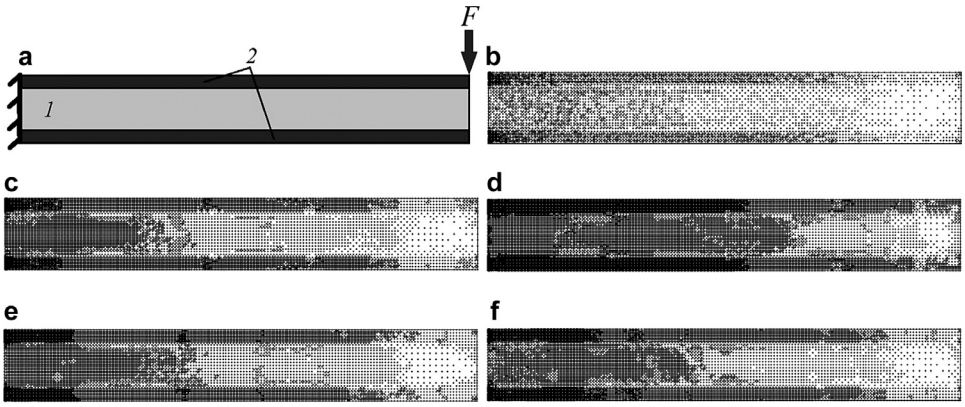

Fig. 4. Loaded structure (computational domain with different material parameters) (a), the resulting nodes of finite-element meshes obtained using the markers m_1 (c), m_2 (d), m_3 (e), m_4 (f), and the reference mesh (b). The materials are concrete (1) and steel (2). Example 2 is illustrated.

adaptive algorithm is $e \leq 3\%$. The same as in the previous example, the m_2 marker leads to excessive mesh splitting. The highest number of algorithm steps for this example occurs when the m_1 marker is used; however, the obtained mesh is close to the reference one by the number of nodes.

Example 3. Let us examine a fixed concrete structure with holes. The respective domain is shown in Fig. 6(a). The body is composed entirely of concrete, with two square holes; the body is fixed along the edge of these holes and in the middle of the bottom side. A distributed load $F = 10^8\,\mathrm{N/m^2}$ is applied from above.

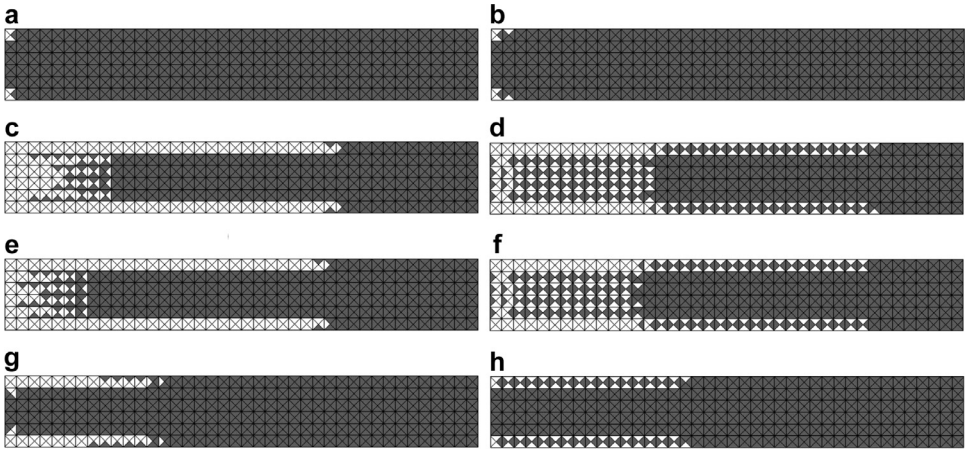

Fig. 5. The elements of the domain (see Fig. 4(a)) selected for splitting (lightly shaded) using different markers: $m_1(\eta_T^{ref})$ (a), $m_1(\eta_T^{\mathrm{RT}})$ (b); $m_2(\eta_T^{ref})$ (c), $m_2(\eta_T^{\mathrm{RT}})$ (d); $m_3(\eta_T^{ref})$ (e), $m_3(\eta_T^{\mathrm{RT}})$ (f); $m_4(\eta_T^{ref})$ (g), $m_4(\eta_T^{\mathrm{RT}})$ (h). Example 2 is illustrated.

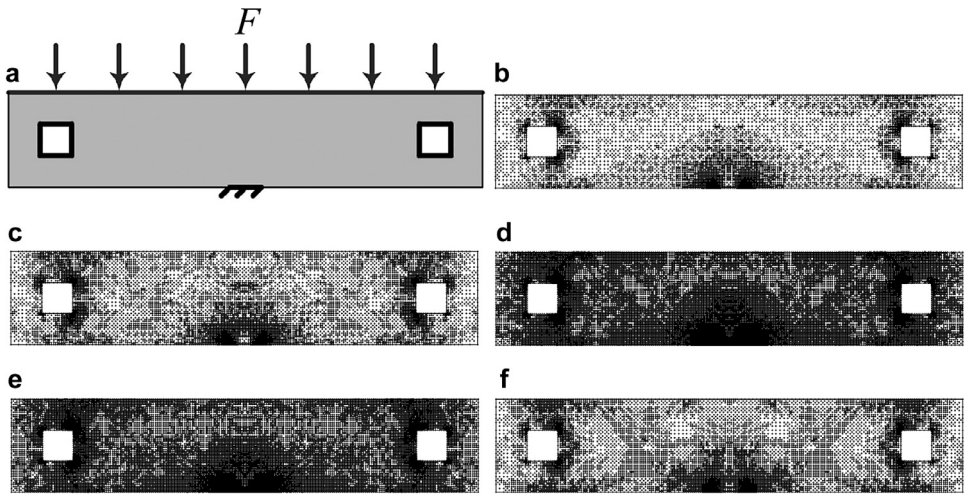

Fig. 6. Loaded concrete structure (computational domain) with holes (a) and the resulting nodes of finite-element meshes obtained using the markers m_1 (c), m_2 (d), m_3 (e), m_4 (f), and the reference mesh (b). Example 3 is illustrated.

Fig. 6 also shows nodes of the reference mesh and of the meshes obtained as a result of adaptations with different markers. Fig. 7 shows the elements selected for splitting on a uniform mesh using the markers computed from the indicators η^{RT} and η^{ref}. The accuracy of the markers on a uniform mesh and the data for the adaptive meshes whose nodes are shown in Fig. 6 are listed in Table 1. The stopping criterion for the adaptive algorithm is $e \leq 4\%$.

It can be seen from Figs. 6 and 7 and from Table 1 that the second and the third markers result in meshes with significantly greater numbers of nodes with the same level of relative error, compared to the markers m_1 and m_4; however, areas of node condensation coincide for all markers. As in the previous examples, a small number of elements is selected at each step using the m_1 marker; because of this, the number of adaptation steps increases (see the third column of Table 1 and Example 3).

5. Conclusion

Four of the most commonly used element-marking criteria were described in the study; these criteria were used in adaptive algorithms for solving plain-strain problems for various materials and geometries.

The results proved that it is necessary to use both the graphical (e.g., resulting meshes and graphs of selected elements) and the quantitative (number of algorithm steps, marker accuracy, number of adaptive

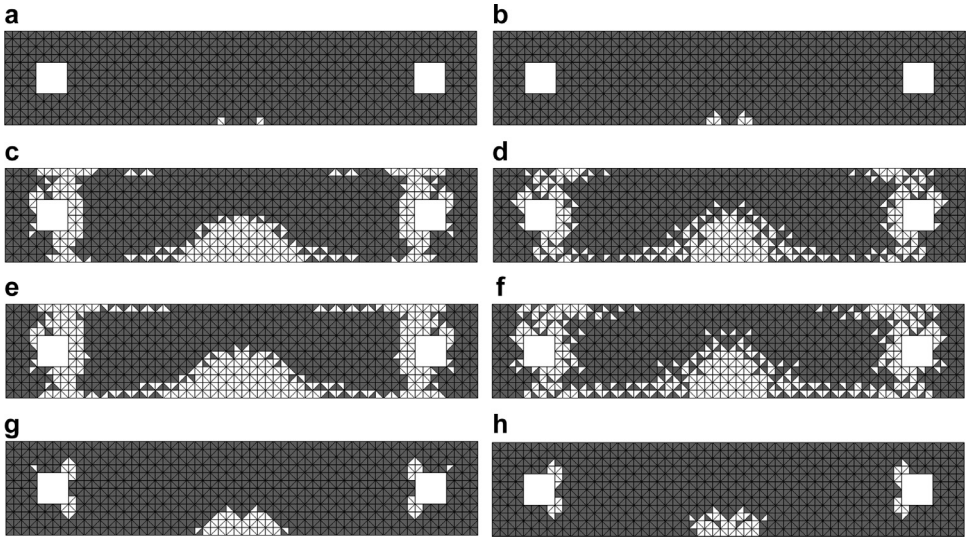

Fig. 7. The elements of the domain (see Fig. 6(a)) selected for splitting (lightly shaded) using different markers: $m_1(\eta_T^{ref})$ (a), $m_1(\eta_T^{\mathrm{RT}})$ (b); $m_2(\eta_T^{ref})$ (c), $m_2(\eta_T^{\mathrm{RT}})$ (d); $m_3(\eta_T^{ref})$ (e), $m_3(\eta_T^{\mathrm{RT}})$ (f); $m_4(\eta_T^{ref})$ (g), $m_4(\eta_T^{\mathrm{RT}})$ (h). Example 3 is illustrated.

mesh nodes) comparison methods in order to choose the criterion for element selection. Using individual criteria does not allow to fully assess the quality of a marker.

It can be concluded from the results obtained that the main areas of node condensation for the resulting adaptive mesh do not depend on the choice of marker. The mesh obtained using the m_1 marker proves to be the closest to the reference one but more adaptation steps are required in this case compared with the other marking criteria. The results for the m_3 marker and the 'bulk criterion' m_4 depend on the selected problem. None of these two criteria could be established to be consistently superior to the others from the examples listed in the paper and the ones considered in the course of solving the problems.

We should note that the number of nodes in the resulting mesh and the number of algorithm steps for the markers m_1 and m_4 depends on the parameter α, and on the number of elements split at a time for the m_3 marker. Selecting these parameters for a specific problem can improve the quality of the obtained adaptive meshes.

Acknowledgment

The study was supported by the Russian Foundation for Basic Research (grant no. 14-01-31273mol_a).

References

[1] A. Muzalevsky, S. Repin, On two-sided error estimates for approximate solutions of problems in the linear theory of elasticity, Russ. J. Numer. Anal. Math. Model. 18 (1) (2003) 65–85.
[2] S. Repin, L.S. Xanthis, A posteriori error estimation for elasto-plastic problems based on duality theory, Comput. Methods Appl. Mech. Eng. 138 (1–4) (1996) 317–339.
[3] S.I. Repin, A Posteriori Estimates For Partial Differential Equations: Radon Series On Computational And Applied Mathematics, de Gruyter, Berlin, 2008.
[4] M. Frolov, Application of functional error estimates with mixed approximations to plane problems of linear elasticity, Comput. Math. Math. Phys. 53 (7) (2013) 1000–1012.
[5] M. Frolov, Implementation of error control for solving plane problems in linear elasticity by mixed finite elements, Comput. Contin. Mech. 7 (1) (2014) 73–81.
[6] M.A. Churilova, M.E. Frolov, Functional a posteriori error estimates for linear elasticity: computational properties and adaptive algorithms, Humanit. Sci. Univ. J 10 (2014) 23–36.
[7] O. Mali, P. Neittaanmäki, S. Repin, Accuracy verification methods. theory and algorithms, Computational Methods in Applied Sciences, Springer, Dordrecht, 2014.
[8] R. Verfürth, A Review of A Posteriori Error Estimation and Adaptive Mesh Refinement Techniques, John Wiley & Sons, Chichester; B.G. Teubner Verlag Stuttgart, 1996.
[9] S. Bertoluzza, R.H. Nochetto, A. Quarteroni, et al., Multiscale and Adaptivity: Modeling, Numerics and Applications. C.I.M.E. Summer School, Cetraro, Italy, Springer-Verlag Berlin Heidelberg, 2012, 2009.